SPANDIDOS PUBLICATIONS

ONCOLOGY LETTERS 15: 6179-6188, 2018

Analysis of H3K27me3 expression and DNA methylation at CCGG sites in smoking and non-smoking patients with non-small cell lung cancer and their clinical significance

KUNSHOU ZHU[1*], YUJIE DENG[2*], GUOXING WENG[3], DAN HU[4], CHENG HUANG[5], KEITARO MATSUMOTO[6], TAKESHI NAGAYASU[6], TAKEHIKO KOJI[7], XIONGWEI ZHENG[4], WENHUI JIANG[4], GEN LIN[5], YIBIN CAI[1], GUIBIN WENG[1] and XIAOHUI CHEN[1]

[1]Department of Oncological Surgery, Fujian Cancer Hospital and Fujian Medical University Cancer Hospital, Fuzhou, Fujian 350014; [2]Department of Chemotherapy, The First Affiliated Hospital of Fujian Medical University, Fuzhou, Fujian 350005; [3]Department of Cardiac Surgery, Fujian Provincial Hospital, Fuzhou, Fujian 350001; Departments of [4]Pathology and [5]Medical Oncology, Fujian Cancer Hospital and Fujian Medical University Cancer Hospital Fuzhou, Fuzhou, Fujian 350014, P.R. China; [6]Division of Surgical Oncology, Department of Translational Medical Sciences, Nagasaki University Graduate School of Biomedical Science, Nagasaki, Nagasaki 852-8501; [7]Department of Histology and Cell Biology, Nagasaki University Graduate School of Biomedical Sciences, Nagasaki, Nagasaki 852-8523, Japan

Received February 10, 2017; Accepted December 4, 2017

DOI: 10.3892/ol.2018.8100

Abstract. Smoking frequently leads to epigenetic alterations, including DNA methylation and histone modifications. The effect that smoking has on the DNA methylation levels at CCGG sites, the expression of trimethylation of histone H3 at lysine 27 (H3K27me3) and enhancer of zeste homolog 2 (EZH2), and their interactions in patients with non-small cell lung cancer (NSCLC) were analyzed. There were a total of 42 patients with NSCLC, 22 with adenocarcinomas and 20 with squamous cell carcinomas enrolled in the present study. Expression of H3K27me3, EZH2 and proliferating cellular nuclear antigen (PCNA) were immunohistochemically detected. DNA methylation at CCGG sites was evaluated via histoendonuclease-linked detection of DNA methylation sites. The apoptotic index of cancerous tissues obtained from patients of different smoking statuses was evaluated via the terminal deoxynucleotidyl-transferase-mediated dUTP-biotin nick end labeling method. The association with clinicopathological data was calculated relative to different smoking statuses. Compared with the non-smokers, smokers with NSCLC exhibited a significantly lower apoptotic index ($P<0.05$), and frequently had a lower level of DNA methylation at CCGG sites, lower H3K27me3 expression and a higher EZH2 expression ($P<0.05$). DNA methylation levels at CCGG sites were negatively correlated to the Brinkman index ($P=0.017$). Furthermore, there was a parallel association between the H3K27me3 and EZH2 expression levels in the majority of smokers, whereas in the majority of non-smokers, there was a diverging association ($P=0.015$). There was a diverging association between the PCNA and EZH2 expression levels in the majority of smokers; however, in the majority of non-smokers, there was a parallel association ($P=0.048$). In addition, the association between the CCGG methylation ratio and immunohistochemical expression of H3K27me3 was a parallel association in the majority of smokers, while in the majority of non-smokers there was a diverging association ($P=0.049$). Conclusively, patients with NSCLC and different smoking statuses exhibit different epigenetic characteristics. Additionally, DNA methylation levels at the CCGG sites may have the ability to determine associations between the expression levels of H3K27me3, EZH2 and PCNA.

Correspondence to: Dr Xiaohui Chen, Department of Oncological Surgery, Fujian Cancer Hospital and Fujian Medical University Cancer Hospital, 420 Fuma Road, Jin'an, Fuzhou, Fujian 350014, P.R. China
E-mail: chenxiaojun13@hotmail.com

*Contributed equally

Abbreviations: NSCLC, non-small cell lung cancer; ADC, adenocarcinoma; SCC, squamous cell carcinoma; H3K27me3, trimethylation of histone H3 at lysine 27; EZH2, enhancer of zeste homolog 2; PRC2, polycomb repressive complex 2; PCNA, proliferating cellular nuclear antigen; TUNEL, terminal deoxynucleotidyl-transferase-mediated dUTP-biotin nick end labeling; HELMET, histoendonuclease-linked detection of methylation sites of DNA

Key words: smoking, DNA methylation, trimethylation of histone H3 at lysine 27, EZH2, non-small cell lung cancer

Introduction

Lung cancer is the leading cause of cancer-associated mortalities in China and globally (1-3). A number of studies have indicated that 85-90% of these cases are a result of voluntary or involuntary (second-hand) smoking (4-7), with a notable

dose-response association (8). Furthermore, numerous studies have demonstrated that inhalation of toxicants, including cigarette smoke, may result in irreversible changes to genetic material, including DNA mutations and putatively reversible changes to the epigenetic landscape, and changes in DNA methylation and the chromatin modification state (9-11).

The tumorigenesis of lung cancer involves genetic and epigenetic alterations, including DNA methylation and histone modifications. One of the most common epigenetic regulations is cytosine methylation, which affects the primary structure of chromatin and its secondary structure, which is critical to the regulation of gene expression (12), as well as the interactions within DNA and histones. Recently, aberrant methylation of CpG islands in the promoter region of tumor suppressor genes (TSGs) has been identified as an important epigenetic mechanism for gene silencing, which may have a limited effect on tumor proliferation and cellular apoptosis for global hypomethylation of genomic DNA and the hypermethylation of gene promoter regions occur simultaneously in a wide variety of malignancies, including lung cancer (8). The aim of the present study was to evaluate the growth and apoptotic index of non-small cell lung cancer (NSCLC) with different smoking statuses.

Histone modification, particularly methylation of lysine may be associated with the transcriptional status of genes and chromatin structure (13). Trimethylated histone H3 at lysine 27, a transcription-suppressive histone modification, is methylated via the enhancer of zeste homolog 2 (EZH2). EZH2, the catalytic subunit of polycomb repressive complex 2 (PRC2), contributes to the maintenance of cell identity, cell cycle regulation and tumorigenesis (14,15). Overexpression of the EZH2 gene occurs in a variety of human malignancies, including breast, prostate, endometrial, gastric, colon, hepatocellular, bladder and oral cancer (16). Recently, a number of studies have reported that trimethylation of histone H3 at lysine 27 (H3K27me3) serves a significant role in the development and/or progression of various human cancer types, including lung cancer (13,17). Theoretically, as the methyltransferase for H3K27me3, the expression of EZH2 should change simultaneously with the expression of H3K27me3; however, a previous study (17) revealed that the association in the expression levels did not match this theory. The underlying mechanism of this paradox remains unknown. It was theorized that cigarette smoking, which frequently results in epigenetic alterations, may have a limited effect on this phenomenon. To date, the expression dynamics of H3K27me3 in lung cancer with different smoking statuses have not been investigated (13).

In the present study, the major gene involved in inactivating histone modification was investigated, including the expression of H3K27me3, and the DNA methylation status at CCGG sites in smoking and non-smoking patients with NSCLC, along with the possible clinical significance.

Materials and methods

Patients and tissue preparation. Archived formalin-fixed paraffin-embedded tissue sections from a series of 42 patients [22 adenocarcinomas (ADC) and 20 squamous cell carcinomas (SCC); 27 males and 15 females; age range, 39-87 years] who had undergone surgical resection for NSCLC at the First Department of Surgery, Nagasaki University Hospital (Nagasaki, Nagasaki) between February 2000 and November 2006 were selected. None had received chemo- or radiotherapy prior to tissue collection. The histopathological features of cancerous specimens were classified in accordance with the 8th American Joint Committee on Cancer criteria on lung cancer, and the TNM staging system (18). The study protocol was approved by the Human Ethics Review Committee of Nagasaki University School of Medicine and signed informed consent was obtained from each patient. Serial sections were cut at a thickness of 4 μm and placed onto 3-aminopropyltriethoxysilane-coated glass slides. A number of sections were stained with hematoxylin and eosin (H&E) in a routine manner for histological examination (19).

Chemicals and biochemicals. Bovine serum albumin (BSA; essentially fatty acid and globulin-free), Trizma base, 2-mercaptoethanol, 3-aminopropyltriethoxysilane and Brij-35 were obtained from Sigma-Aldrich (Merck KGaA, Darmstadt, Germany); 3,3'-Diaminobenzidine-4HCl (DAB) was purchased from Chemical Dojin Co., Ltd. (Kumamoto, Japan). Biotin-16-dUTP, digoxigenin-11-dUTP, Rhodamine anti-Dig and terminal deoxynucleotidyltransferase (TdT) were from Roche Diagnostics (Mannheim, Germany). Dideoxy ATP (ddATP) and dideoxy TTP (ddTTP) were from Jena Bioscience (Jena, Germany). *Hpa*II and *Msp*I were purchased from Takara Bio, Inc. (Otsu, Japan). DAPI was obtained from Invitrogen (Thermo Fisher Scientific, Inc., Waltham, MA, USA). Permount was from Thermo Fisher Scientific, Inc. All other reagents used in the present study were obtained from Wako Pure Chemicals Industries, Inc. (Osaka, Japan) and were of analytical grade.

Immunohistochemistry (IHC). IHC was performed with the indirect enzyme-labeled antibody method, as described previously (17,20-22). All experimental procedures were performed in room temperature unless otherwise indicated. IHC using anti-H3K27me3 polyclonal (1:200; cat. no. 9733) antibody, anti-EZH2 monoclonal (1:400; cat. no. 5246) antibody (both from Cell Signaling Technology, Inc., Danvers, MA, USA) and anti-PCNA monoclonal (PC10; 1:400, cat. no. M0879) antibody (DakoCytomation; Agilent Technologies, Inc., Santa Clara, CA, USA) was performed according to the manufacturer's protocol. For detection, paraffin-embedded sections were deparaffinized with toluene and rehydrated in graded alcohol. Following autoclaving for 15 min at 120˚C in 10 mM citrate buffer (pH 6.0) for antigen retrieval, endogenous peroxidase was inactivated with 0.3% hydrogen peroxide in methanol for 15 min. The sections were then pre-incubated with 500 μg/ml normal goat immunoglobulin G (IgG; cat. no. I-5256, Sigma-Aldrich; Merck KGaA) dissolved in 1% BSA in PBS (pH 7.4) for 1 h, reacted with primary antibodies for 16 h, washed with 0.075% Brij™-35 in PBS, and then incubated with horseradish peroxidase (HRP)-conjugated goat anti-rabbit IgG (H3K27me3/EZH2, 1:200) or HRP-conjugated goat anti-mouse IgG (PCNA) in 1% BSA in PBS for 1 h (cat. no. AP307P; EMD Millipore, Billerica, MA, USA). Following washing with 0.075% Brij™-35 in PBS, the sites of HRP were visualized with DAB and H_2O_2 in the presence of nickel, and cobalt ions (23). As a negative control, a number of sections were reacted with normal rabbit IgG or normal mouse

IgG (1:500; cat. nos. X-0903 and X-0931, respectively, both Dako Cytomation; Agilent Technologies, Inc.) instead of the specific antibodies.

Quantitative evaluation. Staining results were examined by two pathologists (D. Hu and W. Jiang) blinded to the clinical information of patients. Another reading by a third observer was needed to reach a consensus when there was a significant discrepancy between initial readings. At least five high-power fields and >2,000 cells were analyzed in each case with a Zeiss 2021-85 light microscope (Carl Zeiss AG, Oberkochen, Germany) at x400 magnification. Immunostaining results were evaluated via a semi-quantitative scoring system as previously described (24), and the final score ranged from 0-12.

TdT-mediated dUTP nick end labeling (TUNEL) staining for apoptotic cancerous cells in NSCLC with different smoking statuses. To identify nuclei with DNA strand breaks at a cellular level, TUNEL was performed according to the method by Gavrieli *et al* (25). In brief, paraffin sections (5 μm) were cut onto silane-coated glass slides, dewaxed with toluene and rehydrated in an ethanol series. Following washing with PBS, the sections were treated with 5 μg/ml and of proteinase K (Takara Bio, Inc.) in PBS at 37˚C for 15 min. The sections were then washed once with deionized distilled water and incubated with TdT buffer (25 mM Tris/HCl buffer, pH 6.6, containing 0.2 M potassium cacodylate and 0.25 mg/ml BSA) alone at room temperature for 30 min. Following incubation, the slides were reacted with 200 U/ml TdT dissolved in TdT buffer, supplemented with 5 μM biotin-16-dUTP, 20 μM dATP, 1.5 mM $CoCl_2$ and 0.1 mM dithiothreitol, at 37˚C for 1 h. The reaction was terminated by washing with 50 mM Tris/HCl buffer (pH 7.4) for 15 min. Endogenous peroxidase activity was inhibited by immersing the slides in 0.3% H_2O_2 in methanol at room temperature for 15 min. The signals were detected immunohistochemically with a HRP-conjugated goat anti-biotin antibody (1:100, cat. no. AP132B; EMD Millipore), as described previously (17,22). For statistical analysis, >10,000 cancer cells/patient were counted, and the number of TUNEL-positive cells was expressed per 1,000 of the total cells (mean ± standard error of the mean). Data for different groups were compared for statistical differences using the Student's t-test. $P<0.05$ was considered to indicate a statistically significant result.

In situ evaluation of DNA methylation. To evaluate the DNA methylation level of NSCLC at the CCGG sites, histoendonuclease-linked detection of methylation sites of DNA (HELMET) was performed (17,26). Paraffin sections were dewaxed and digested with 10 μg/ml proteinase K in PBS at 37˚C for 15 min. Then the sections were incubated with TdT buffer alone at room temperature for 30 min. Following incubation, the slides were reacted with 800 U/ml TdT dissolved in TdT buffer containing 20 μM ddATP, 20 μM ddTTP, 1.5 mM $CoCl_2$ and 0.1 mM dithiothreitol at 37˚C for 2 h. Following washing with PBS, the sections were fixed with freshly-prepared 4% paraformaldehyde (PFA) in PBS for 5 min at room temperature and then rinsed with PBS. The non-methylated CCGG sites were digested at 37˚C for 2 h with 100 U/ml *Hpa*II dissolved in 10 mM Tris/HCl buffer (pH 7.5), containing 10 mM $MgCl_2$ and 1 mM dithiothreitol. The *Hpa*II-cut sites were labeled with biotin-16-dUTP via TdT reaction for 90 min at 37˚C. Then, the 3'-OH ends were blocked with a mixture of dideoxynucleotides by TdT at 37˚C as aforementioned, for 2 h. Following fixation with 4% PFA in PBS, the methylated CCGG sites were digested at 37˚C for 2 h by 100 U/ml *Msp*I dissolved in Tris/HCl buffer (pH 7.9), containing 10 mM $MgCl_2$, 0.5 mM dithiothreitol, 66 mM potassium acetate and 0.1% BSA. The *Msp*I-cut sites were then labeled with digoxigenin-11-dUTP via TdT reaction for 90 min at 37˚C. Finally, the sections were incubated with a mixture of 500 μg/ml normal goat IgG and normal sheep IgG (cat. no. B3148; Sigma-Aldrich; Merck KGaA) in 5% BSA/PBS for 1 h at 37˚C, and then visualized by fluorescein isothiocyanate-labeled goat anti-biotin and rhodamine-labeled sheep anti-digoxigenin (both 1:100, cat. no. SP-3040; Vector Laboratories, Ltd., Peterborough, UK; and cat. no. 11082736103 from Roche Diagnostics) for 1 min. The nuclei were stained with 0.5 μg/ml DAPI for 1 min at room temperature. The stained slides were analyzed under a laser scanning microscope (x400 magnification, LSM 5 PASCAL; Zeiss GmbH, Jena, Germany).

Statistical analysis. The X-tile software program version 3.6.1 (Yale University School of Medicine, New Haven, CT, USA), described previously (27), was used to determine the threshold value of H3K27me3 for classifying samples into groups of high and low expression. The SPSS statistical software package (version 23; IBM Corp., Armonk, NY, USA) was employed for all analyses. The association between markers, and the clinicopathological characteristics of the patients, either separated or combined, including age, sex, tissue type, tumor differentiation, P-factor, LV-factor, V-factor, smoking status, Brinkman index, CCGG methylation ratio, relapse, postoperative metastasis and carcinoembryonic antigen (CEA) level, were evaluated by the Pearson's χ^2 and Fisher's exact tests, or Spearman's rank correlation as appropriate. $P<0.05$ was considered to indicate a statistically significant difference.

Results

Clinicopathological data of patients. The clinicopathological data of the patients with cancer are depicted in Table I. The cohort included 27 males and 15 females, with a mean age of 69 years. By histological classification, 20 cases were SCC and 22 were ADE. In the SCC group, the number of well-, moderately- and poorly-differentiated cancer types were 3, 9, and 8, respectively. In the ADE group, the number of cancer types with predominant growth patterns for lepidic, acinar, papillary and solid with mucin were 7, 6, 4 and 5, respectively. All cases were TNM stage 1 and lymph node-negative. Postoperative follow-up data were available in all cases, and the median follow-up duration in the ADC and SCC groups were 75.2, and 52.9 months, respectively.

As depicted in Table I, among the 42 patients with lung cancer, the majority of the smokers were male (21/27), whereas the majority of females (12/15) did not smoke. SCC was predominant in smokers (20/20), whereas ADE was the main histological type in non-smokers (15/22); therefore, smoking resulted in a ≥2-fold higher risk of SCC than ADE (20:7).

Table I. Clinicopathological data of patients.

Parameter	No. of cases (%)	
	ADC	SCC
Median age, years	68.50	69.75
Age, years		
≤69	12 (54.5)	12 (60)
>69	10 (45.5)	8 (40)
Sex		
Male	10 (45.5)	17 (85)
Female	12 (54.5)	3 (15)
Serum CEA, ng/ml		
≤5	22 (100)	17 (85)
>5	0	3 (15)
P-factor		
Positive	1 (4.5)	0
Negative	21 (95.5)	20 (100)
LV-factor		
Positive	18 (81.8)	13 (65)
Negative	4 (18.2)	7 (35)
V-factor		
Positive	8 (36.4)	10 (50)
Negative	14 (63.6)	10 (50)
T-stage		
1a	16 (72.7)	13 (65)
1b	5 (22.7)	7 (35)
2a	1 (4.6)	
Nodal status		
N0	22 (100)	20 (100)
Differentiation (SCC)		
Well		3 (15)
Moderate		9 (45)
Poor		8 (40)
Predominant growth pattern (ADC)		
Lepidic	7 (31.8)	
Acinar	6 (27.3)	
Papillary	4 (18.2)	
Solid with mucin	5 (22.7)	
Relapse		
Yes	2 (9.1)	8 (40)
No	20 (90.9)	12 (60)
Smoking status		
Smoker	7 (31.8)	20 (100)
Non-smoker	15 (68.2)	0 (0)
Postoperative metastasis		
Yes	3 (13.6)	7 (35)
No	19 (86.4)	13 (65)
Median follow-up, months	75.2	52.9

ADC, adenocarcinoma; SCC, squamous cell carcinoma; CEA, carcinoembryonic antigen; P-factor, the status of tumor invasion into the visceral pleura; LV-factor, the status of tumor invasion into the lymphatic vessels; V-factor, the status of tumor invasion into the veins.

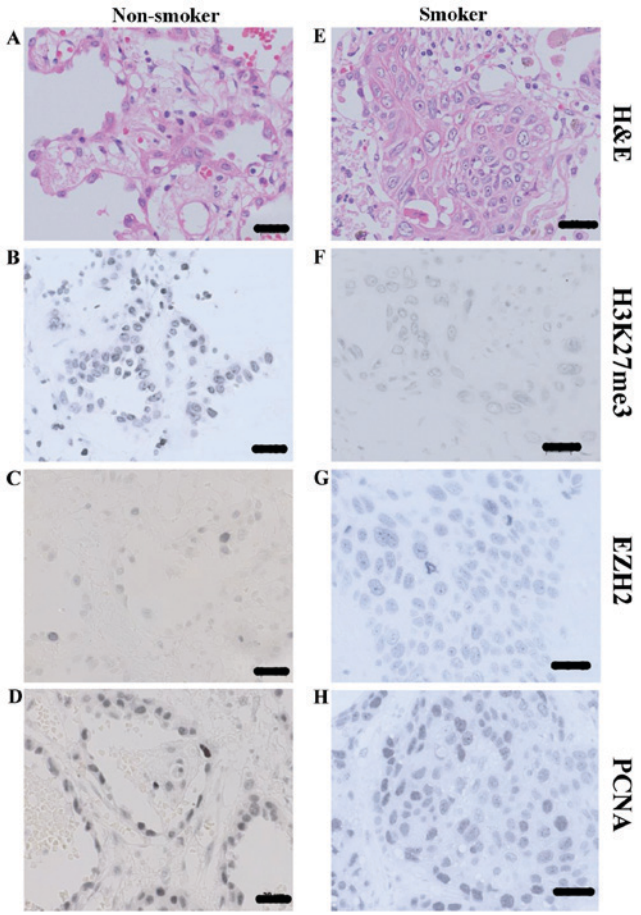

Figure 1. Immunostaining for H3K27me3, EZH2 and PCNA in NSCLC tissues of smoking and non-smoking patients. (A) H&E staining for NSCLC tissues of non-smoking patients. (B) Strong expression of H3K27me3 in NSCLC tissues of non-smoking patients. (C) Weak staining of EZH2 in NSCLC tissues of non-smoking patients. (D) PCNA expression in NSCLC tissues in non-smoking patients. (E) H&E staining for NSCLC tissues of smoking patients. (F) Weak expression of H3K27me3 in NSCLC tissues of smoking patients. (G) Strong staining of EZH2 in NSCLC tissue of smoking patients. (H) PCNA expression in NSCLC tissues of smoking patients. Scale bar, 20 μm. NSCLC, non-small cell lung cancer; H3K27me3, trimethylation of histone H3 at lysine 27; EZH2, enhancer of zeste homolog 2; PCNA, proliferating cellular nuclear antigen; H&E, hematoxylin and eosin.

Expression of H3K27me3, EZH2 and PCNA in NSCLC tissues of smoking and non-smoking patients. The NSCLC tissues from smokers and non-smokers were stained using various antibodies in order to determine the expression H3K27me3, EZH2, and PCNA (Fig. 1). H&E staining of NSCLC tissue demonstrated the normal status of histological status used in the present study (Fig. 1A and E). H3K27me3, EZH2 and PCNA were all predominantly localized in the nuclei in NSCLC (Fig. 1B-D and F-H). The calculated staining score of immunopositive cells for H3K27me3 and EZH2 ranged from 0-12 in all tested tissues, whereas PCNA staining was expressed as a percentage of immunopositive cells. According to the X-tile plots (data not shown), the samples were categorized into low (IHC score ≤3) and high (IHC score >3) expression subgroups for H3K27me3, based on a cutoff point determined by X-tile software associated with survival status. As for EZH2 and PCNA, the average score was used to evaluate their expression level. As depicted in Figs. 1B, F and 2A, the staining score of H3K27me3 was significantly higher in non-smoker NSCLC tissue, compared

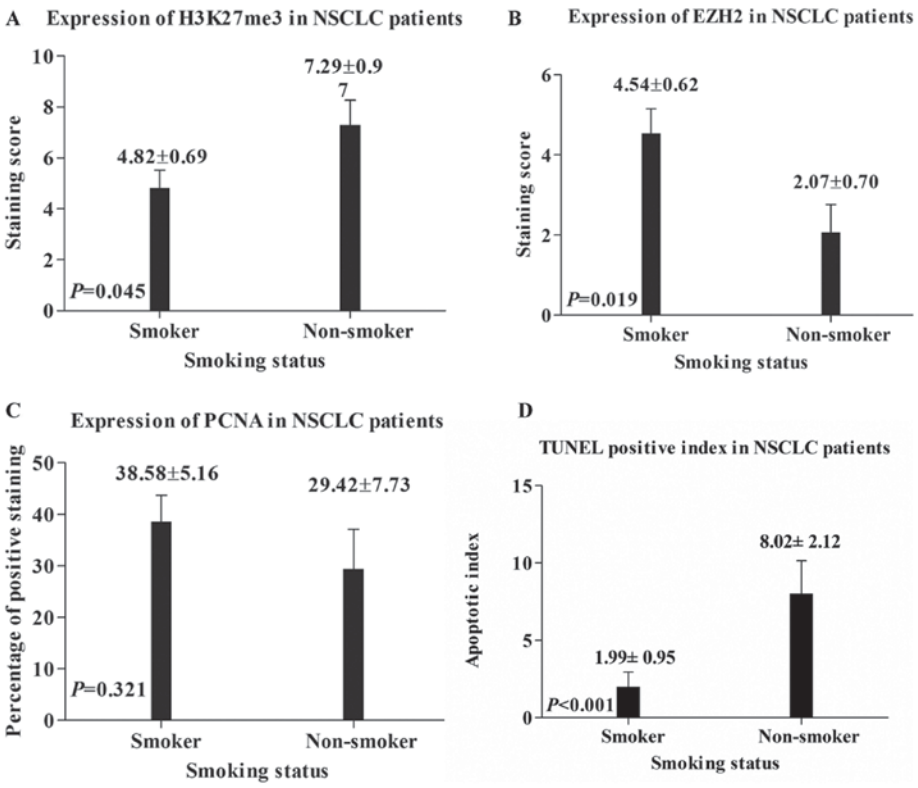

Figure 2. (A) Trimethylation of histone H3 at lysine 27 expression levels differed in NSCLC patients with various smoking statuses (P=0.045). (B) Enhancer of zeste homolog 2 expression levels differed in NSCLC patients with various smoking statuses (P=0.045). (C) No difference in the proliferating cellular nuclear antigen expression levels in NSCLC patients with various smoking statuses (P=0.321). (D) A notable difference in the terminal deoxynucleotidyl-transferase-mediated dUTP-biotin nick end labeling apoptotic index between smoking and non-smoking patients was observed (8.02±2.12 vs. 1.99±0.95; P<0.001). NSCLC, non-small cell lung cancer; H3K27me3, trimethylation of histone H3 at lysine 27; EZH2, enhancer of zeste homolog 2; PCNA, proliferating cellular nuclear antigen; TUNEL, terminal deoxynucleotidyl-transferase-mediated dUTP-biotin nick end labeling.

within those of smokers (7.29±0.97 vs. 4.82±0.69; P=0.045); however, the staining score of EZH2 was significantly higher in smoker NSCLC tissue, compared within those of non-smokers (4.54±0.62 vs. 2.07±0.70; P=0.019; Figs. 1C, G and 2B). No statistical significance was determined between the PCNA expression in smoker and non-smoker NSCLC tissues (38.58±5.16 vs. 29.42±7.73; P=0.321; Figs. 1D, H and 2C).

Apoptotic evaluation in patients with NSCLC with different smoking status. In comparison to smoking patients with NSCLC, a higher apoptotic index was observed in non-smokers (8.02±2.12 vs. 1.99±0.95; P<0.001; Fig. 2D). Fig. 3A and B demonstrated the normal status of tissue used for TUNEL evaluation. In each case, cells with the morphological characteristics of apoptosis were identified by: Chromatin condensation; the formation of crescentic caps of condensed chromatin at the nuclear periphery; and the formation of visible apoptotic bodies (arrows in Fig. 3C and D).

DNA methylation level at CCGG sites and its association with clinicopathological parameters. As depicted in Table II, CCGG sites in non-smokers with NSCLC were generally hypermethylated, compared with those of smokers (P=0.016). Furthermore, due to the non-normal distribution of the Brinkman index and the methylation ratio at CCGG sites, Spearman's rank correlation analysis (data not shown) was used to determine the correlation, and a notable statistical significance was determined (P=0.017).

Correlation between smoking status and other clinicopathological parameters in patients with NSCLC. As indicated in Table II, in comparison with non-smokers, smokers exhibited significantly lower H3K27me3 expression (P=0.029), a lower methylation ratio at CCGG sites (P=0.016) and higher EZH2 expression (P=0.029). When evaluating the trends in the expression or alterations to multiples factors, it was identified that a parallel association between the H3K27me3 and EZH2 expression levels in the majority of smoking patients with NSCLC, while in non-smoking patients with NSCLC, the majority of their expression levels were not significant (P=0.015). There was a diverging association between PCNA and EZH2 expression levels in the majority of smoking patients with NSCLC, while in most non-smoking patients with NSCLC their expression levels identified statistical significance (P=0.048). Figs. 4 and 5 depict 4 patients with different smoking statuses. Patients A and B were smokers, whereas patients C and D were non-smokers. Tissue samples from each patient were stained with H&E, H3K27me3, EZH2 and PCNA. It was determined that patients with NSCLC and differing smoking statuses had distinct immunostaining for H3K27me3, EZH2 and PCNA. IHC staining of H3K27me3, EZH2 and PCNA for patients A and B were all high (Fig. 4A, panels 2-4), and all low (Fig. 4B, panels 2-4), respectively. While IHC staining of H3K27me3, EZH2 and PCNA for patients C and D were high, low and low (Fig. 5A, panels 2-4), and low, high and high (Fig. 5B, panels 2-4), respectively. In addition, the association between the CCGG methylation ratio and the immunohistochemical expression of H3K27me3 was

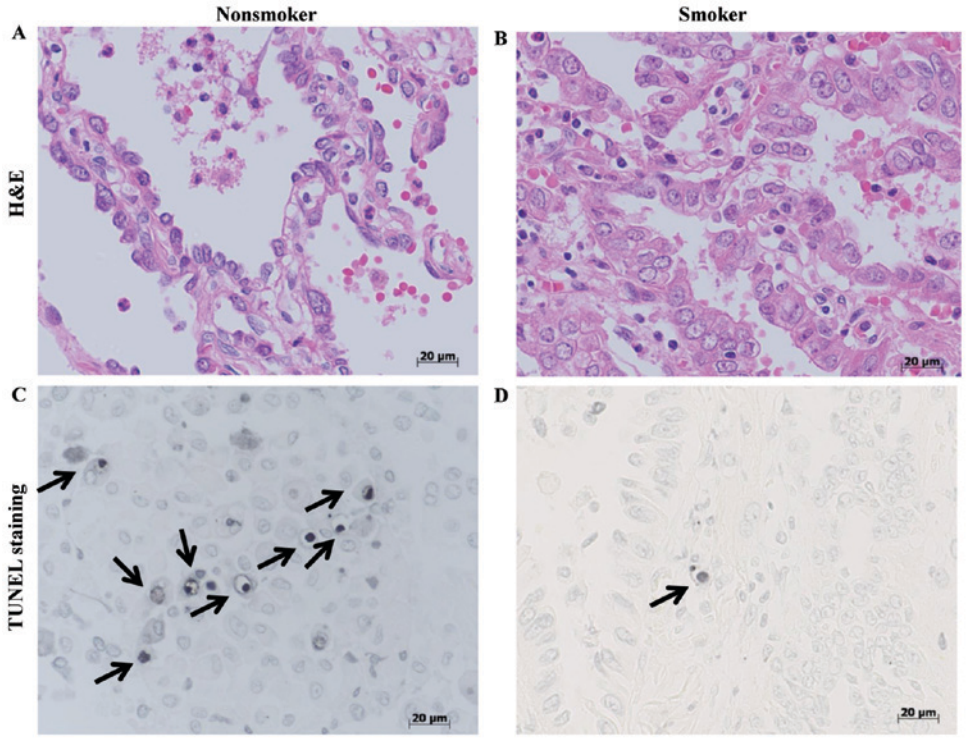

Figure 3. Apoptotic tumor cells stained by (A and B) hematoxylin and eosin and (C and D) terminal deoxynucleotidyl-transferase-mediated dUTP-biotin nick end labeling for non-small cell lung cancer tissues of smoking and non-smoking patients. The arrows indicate apoptotic tumor cells in non-smoker and smoker characterized by chromatin condensation, formation of crescentic caps of condensed chromatin at the nuclear periphery and formation of apoptotic bodies. Scale bar, 20 μm. TUNEL, terminal deoxynucleotidyl-transferase-mediated dUTP-biotin nick end labeling; H&E, hematoxylin and eosin.

parallel in the majority of smoking patients with NSCLC, while in the majority of non-smoking patients with NSCLC there was a diverging association (P=0.049). There was an association between the CCGG methylation ratio and the immunohistochemical expression of EZH2 (P=0.050), between the CCGG methylation ratio and the immunohistochemical expression of PCNA (P=0.382) and between H3K27me3 and PCNA expression (P=0.331), in patients with NSCLC with different smoking statuses; however, the associations were identified as having a low significance (Table II). In addition, no statistical significance was demonstrated between smoking status and the involvement of the lymphatic vessels (P=0.731), pulmonary vein (P=0.280), visceral pleura (P=0.429), PCNA expression (P=0.375) and serum CEA level (P=0.247).

Discussion

In the present study, epigenetic characteristics, including histone modification and DNA methylation, in NSCLC were investigated. Additionally, tumor proliferation, as well as its apoptotic index in smoking and non-smoking patients with NSCLC were evaluated. This demonstrated that a lower expression level of H3K27me3 and a lower level of DNA methylation at CCGG sites were predominant in smoking patients with NSCLC. In addition, a higher expression level of EZH2 and a lower apoptotic index had been observed in smoking patients with NSCLC, in comparison with those who never smoked; however, no significant difference had been observed in PCNA expression between two groups.

A previous study demonstrated that patients with NSCLC and higher expression of H3K27me3 had an increased overall survival time; therefore, H3K27me3 was demonstrated to be an independent prognostic risk factor (17). The epigenetic changes concerning the effect that tobacco smoking may have on epigenetic modifications, as well as its influence on cellular growth and apoptosis was examined in the present study.

Environmental factors, particularly cigarette smoking, have been implicated in the development and progression of lung cancer by eliciting DNA methylation changes (8). The main epigenetic change in mammals is the aberrant methylation of CpG islands in the gene promoter region. As previously identified, global hypomethylationis an early indicator for colon, lung and breast cancer, and chronic lymphocytic leukemia, and lung cancer as well (11,28). On the contrary, Digel and Lübbert (29) reported that gene hypermethylation was an early event in the process of lung cancer tumorigenesis. These paradoxical results may be better interpreted as different degrees of methylation in various genes, inside or outside the CpG islands. However, in the present study, the DNA methylation levels at CCGG sites were evaluated through the HELMET method, which demonstrated that hypomethylation at CCGG sites was more common in smoking patients with NSCLC (P=0.016), compared with in non-smokers. In addition, a decrease in methylation levels at CCGG sites was determined to closely correlate with a greater Brinkman index (P=0.017), which was an indicator for heavy smoking. Patients with NSCLC and different smoking statuses exhibited varying epigenetic markers, which was revealed via immunohistochemical detection of several major markers, including H3K27me3, EZH2 and PCNA. In addition to a lower methylation level at the CCGG sites, the majority of smoking patients with NSCLC had lower H3K27me3 expression levels and higher expression levels of EZH2. Due to the

Table II. Significance and correlations of clinicopathological data in patients with NSCLC with different smoking status.

Variable	Smoking status		P-value
	Smokers	Non-smokers	
H3K27me3 expression[b,c]			0.029
High	10	14	
Low	14	4	
CCGG methylation ratio[a]			0.016
High	7	12	
Low	17	6	
EZH2 expression[a,b]			0.029
High	14	4	
Low	10	14	
Sex[b]			0.001
Male	21	6	
Female	3	12	
Histology type[b]			0.001
SCC	17	3	
ADC	7	15	
Trend of H3K27me3[c] and EZH2 expression[a,b]			0.015
Parallel association	13	1	
Diverging association	15	13	
Trend of EZH2[a] and PCNA expression[a,b]			0.048
Parallel association	12	11	
Diverging association	16	3	
Trend of H3K27me3[c] and PCNA expression[a,b]			0.331
Parallel association	13	4	
Diverging association	15	5	
CCGG methylation ratio[a] and H3K27me3 expression[c]			0.049
Parallel association	17	8	
Diverging association	11	6	
CCGG methylation ratio[a] and EZH2 expression[a,b]			0.050
Parallel association	11	5	
Diverging association	17	9	
CCGG methylation ratio[a] and PCNA expression[a]			0.382
Parallel association	16	6	
Diverging association	12	8	
Lymphatic vessel involved[b]			0.731
Yes	17	14	
No	7	4	
Pulmonary vein involved			0.280
Yes	12	6	
No	12	12	
Visceral pleura involved[b]			0.429
Yes	0	1	
No	24	17	
PCNA expression[a,b]			0.375
High	22	14	
Low	2	4	
Serum CEA level[b]			0.247
High	3	0	
Low	21	18	

[a]Mean score/ratio; [b]Fisher's exact tests (2-sided); χ^2 test for all the other analyses; [c]cut-point determined by X-tile software. ADC, adenocarcinoma; SCC, squamous cell carcinoma; CEA, carcinoembryonic antigen; PCNA, proliferating cell nuclear antigen; H3K27me3, trimethylation of histone H3 at lysine 27; EZH2, enhancer of zeste homolog 2.

methyltransferase of histone H3 lysine 27, the expression of EZH2 was theorized to be associated with the expression of H3K27me3; however, using a mirror section technique, a diverging association was identified between the EZH2 and H3K27me3 expression levels in the previous investigation (17). It has been repeatedly reported that mutation in the EZH2 gene is a common phenomenon in a variety of cancer types (30,31), including breast and lung cancer. Due to the alteration of methylation status at CCGG sites predominantly identified in smokers, it was hypothesized that low H3K27me3 expression may result from a mutated EZH2, which had lost its catalyzing function in the methylation of H3K27 (32,33). To further investigate the underlying mechanisms, it was theorized that the alteration of DNA methylation levels, resulting from tobacco smoking, would cause modifications in the epigenetic changes. The expression pattern of H3K27me3 and EZH2 in patients with NSCLC with different smoking statuses were further analyzed, and it was determined that there was a parallel association between H3K27me3 and EZH2 expression levels in the majority of smoking patients with NSCLC, whether it was an increase or a decrease; however, in non-smoking patients with NSCLC, the majority of the expression levels had no significant association (P=0.015), indicating that NSCLC tissues from of non-smoking patients with high H3K27me3 expression would present with low EZH2 expression, and *vice versa*. These results could assist in deciphering the phenomenon observed in a previous study (17).

Alterations in the status of DNA methylation, as well as histone modifications, frequently lead to changes in a number of specific genes, including oncogenes and TSGs, resulting in proliferation or apoptosis. This was assessed by means of the immunohistochemical expression of PCNA as well as the TUNEL apoptotic index, in the present study. This study has demonstrated a significantly greater apoptotic index in non-smoking patients with NSCLC tissues, compared with smokers, while no statistical difference was observed between the PCNA expression levels of the two groups. This demonstrated that smoking could facilitate the majority of cancerous cells to obtain cellular immortality, although their proliferative ability may not have differed notably.

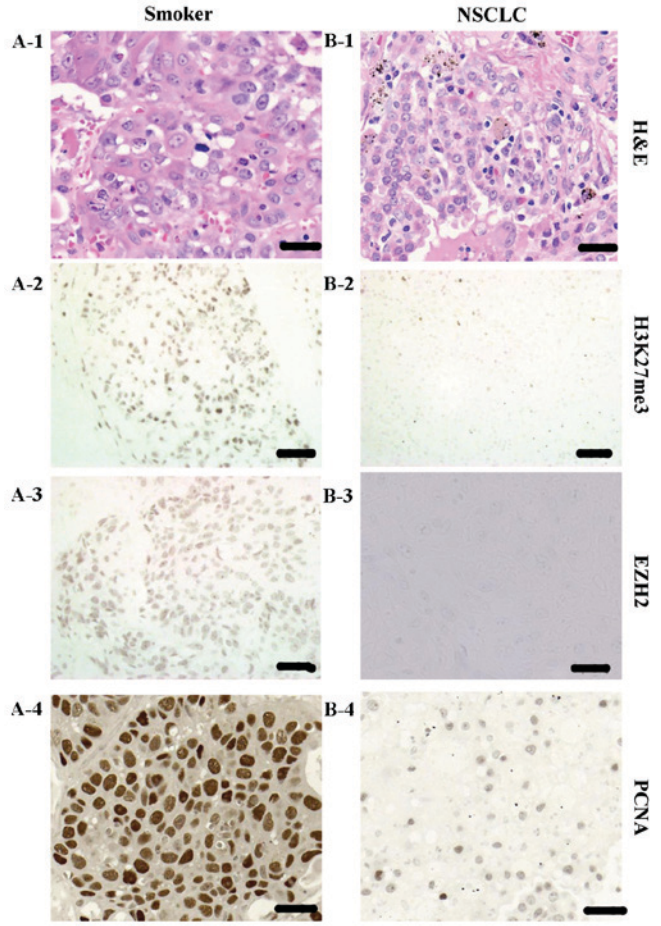

Figure 4. Non-small cell lung cancer tissues of smoking patients stained with (A-1 and B-1) H&E; (A-2 and B-2) H3K27me3; (A-3 and B-3) EZH2; (A-4 and B-4) and PCNA. In accordance with the scoring system aforementioned, patient A exhibited strong (A-2) H3K27me3 expression, (A-3) strong EZH2 expression and (A-4) strong PCNA expression. Patient B exhibited (B-2) weak H3K27me3 expression, (B-3) weak EZH2 expression and (B-4) weak PCNA expression. Scale bar, 20 μm. NSCLC, non-small cell lung cancer; H3K27me3, trimethylation of histone H3 at lysine 27; EZH2, enhancer of zeste homolog 2; PCNA, proliferating cellular nuclear antigen; H&E, hematoxylin and eosin.

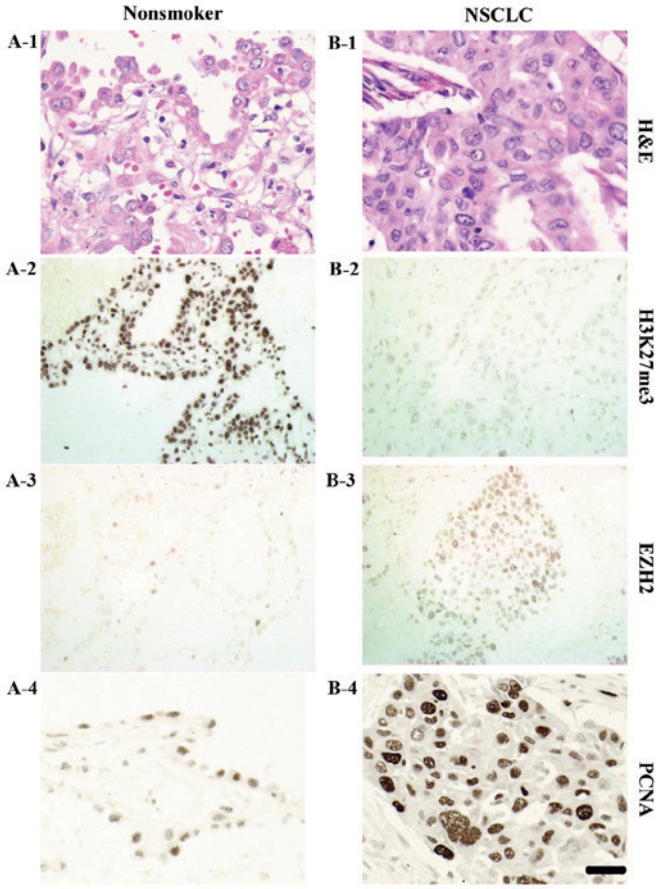

Figure 5. Non-small cell lung cancer tissues of smoking patients stained with (A-1 and B-1), H3K27me3, EZH2(c) H&E; (A-2 and B-2) H3K27me3; (A-3 and B-3) EZH2; and (A-4 and B-4) PCNA. Patient C exhibited strong (A-2) H3K27me3 expression, weak (A-3) EZH2 expression and weak (A-4) PCNA expression. Patient D exhibited weak (B-2) H3K27me3 expression, strong (B-3) EZH2 expressionand strong (B-4) PCNA expression. Scale bar, 20 μm. NSCLC, non-small cell lung cancer; H3K27me3, trimethylation of histone H3 at lysine 27; EZH2, enhancer of zeste homolog 2; PCNA, proliferating cellular nuclear antigen; H&E, hematoxylin and eosin.

Changes in the levels of histone modification, as well as DNA methylation, directly influence disease prognosis. Site-specific histone modifications at H3K27me3 influence the clinical outcome of patients with early-stage NSCLC. Based on published reports (34-36), the novel cigarette smoking-induced site-specific histone and DNA methylation markers identified in the present study will have a greater translational impact on understanding the pathogenetic process involved in smoking-mediated lung disease, including lung cancer and other cancer types. The result demonstrated a coexistence of the alteration of DNA methylation and H3K27me3 expression levels in patients with NSCLC, which is consistent with the study by Takeshima *et al* (37), which is identified specifically in cancer cells and may be used as a target for epigenetic therapy. Analysis of DNA methylation and H3K27me3 expression levels in human colon, breast and prostate cancer cell lines revealed that ~1/4 of DNA methylated genes underwent DNA methylation and H3K27me3 dual modification in cancer cells, while there was a presence of ~1/10 in normal cells.

A number of limitations in the present study should be mentioned. The sample size was limited, which may have led to bias. Further studies with larger sample sizes are required in order to validate the present results, and to identify DNA methylation patterns in specific genes and their associations with histone modifications.

Conclusively, these results indicated that cigarette smoking in patients with NSCLC may lead to lower levels of DNA methylation at CCGG sites, lower H3K27me3 expression levels and a lower cellular apoptotic index. In addition, patients with NSCLC with different smoking statuses exhibited distinct changes in epigenetic markers, which would facilitate the design of epigenetic drugs targeting specific biomarkers for the immortality of cancerous cells.

Acknowledgements

The abstract of this study was presented at the ASCO Annual Meeting 2-6 June 2017 in Chicago, IL, USA and published as abstract no. e23179 in J Clin Oncol 35: 2017.

Funding

This study was supported in part by a Grant-in-Aid for Youth Research Project from Health Administration of Fujian Province

(grant no. 2013-1-10 to X. CHEN), the Fujian Provincial Foundation of Natural Science (grant no. 2016J01515 to X. CHEN), Fujian Medical University Startup Program (grant no. 2016QH040 to Y. DENG) and Fujian Medical University Miaopu Program (grant no. 2015MP032 to Y. DENG).

Availability of data and materials

The analyzed data sets generated during the study are available from the corresponding author, on reasonable request.

Author contributions

Conception and design, KSZ, YJD, TK, XHC; administrative support, XWZ, GXW, KSZ; provision of study materials or patients, KM, TN, TK, XHC; collection and assembly of data, KSZ, YJD, DH, CH, WHJ, GL, YBC, GBW, XHC; data analysis and interpretation, KSZ, YJD, GXW, XWZ, XHC; manuscript writing, all authors; final approval of manuscript, all authors.

Ethics approval and consent to participate

The protocol of this study was approved by the Human Ethics Review Committee of Nagasaki University School of Medicine, and signed informed consent was obtained from all patients.

Consent for publication

Not applicable.

Competing interests

The authors declare that they have no competing interests.

References

1. Chen W, Zheng R, Baade PD, Zhang S, Zeng H, Bray F, Jemal A, Yu XQ and He J: Cancer statistics in China, 2015. CA Cancer J Clin 66: 115-132, 2016.
2. Torre LA, Siegel RL and Jemal A: Lung cancer statistics. Adv Exp Med Biol 893: 1-19, 2016.
3. Siegel RL, Miller KD and Jemal A: Cancer statistics, 2016. CA Cancer J Clin 66: 7-30, 2016.
4. Hussain SP and Harris CC: Molecular epidemiology of human cancer. Recent Results Cancer Res 154: 22-36, 1998.
5. Piyathilake CJ, Frost AR, Bell WC, Oelschlager D, Weiss H, Johanning GL, Niveleau A, Heimburger DC and Grizzle WE: Altered global methylation of DNA: An epigenetic difference in susceptibility for lung cancer is associated with its progression. Hum Pathol 32: 856-862, 2001.
6. Soria JC, Rodriguez M, Liu DD, Lee JJ, Hong WK and Mao L: Aberrant promoter methylation of multiple genes in bronchial brush samples from former cigarette smokers. Cancer Res 62: 351-355, 2002.
7. Wistuba II, Mao L and Gazdar AF: Smoking molecular damage in bronchial epithelium. Oncogene 21: 7298-7306, 2002.
8. Jin Y, Xu P, Liu X, Zhang C, Tan C, Chen C, Sun X and Xu Y: Cigarette smoking, BPDE-DNA adducts, and aberrant promoter methylations of tumor suppressor genes (TSGs) in NSCLC from Chinese population. Cancer Invest 34: 173-180, 2016.
9. Tessema M, Yingling CM, Liu Y, Tellez CS, Van Neste L, Baylin SS and Belinsky SA: Genome-wide unmasking of epigenetically silenced genes in lung adenocarcinoma from smokers and never smokers. Carcinogenesis 35: 1248-1257, 2014.
10. Sundar IK, Nevid MZ, Friedman AE and Rahman I: Cigarette smoke induces distinct histone modifications in lung cells: Implications for the pathogenesis of COPD and lung cancer. J Proteome Res 13: 982-996, 2014.
11. Søes S, Daugaard IL, Sørensen BS, Carus A, Mattheisen M, Alsner J, Overgaard J, Hager H, Hansen LL and Kristensen LS: Hypomethylation and increased expression of the putative oncogene ELMO3 are associated with lung cancer development and metastases formation. Oncoscience 1: 367-374, 2014.
12. Bjaanaes MM, Fleischer T, Halvorsen AR, Daunay A, Busato F, Solberg S, Jørgensen L, Kure E, Edvardsen H, Børresen-Dale AL, *et al*: Genome-wide DNA methylation analyses in lung adenocarcinomas: Association with EGFR, KRAS and TP53 mutation status, gene expression and prognosis. Mol Oncol 10: 330-343, 2016.
13. Wiles ET and Selker EU: H3K27 methylation: A promiscuous repressive chromatin mark. Curr Opin Genet Dev 43: 31-37, 2017.
14. Yu Q, Liu Y, Zheng X, Zhu Q, Shen Z, Wang H, He H, Lin N, Jiang H, Yu L and Zeng S: Histone H3 lysine 4 Trimethylation, lysine 27 trimethylation, and lysine 27 acetylation contribute to the transcriptional repression of solute carrier family 47 member 2 in renal cell carcinoma. Drug Metab Dispos 45: 109-117, 2017.
15. Yang X, Li F, Konze KD, Meslamani J, Ma A, Brown PJ, Zhou MM, Arrowsmith CH, Kaniskan HÜ, Vedadi M and Jin J: Structure-activity relationship studies for enhancer of zeste homologue 2 (EZH2) and enhancer of zeste homologue 1 (EZH1) inhibitors. J Med Chem 59: 7617-7633, 2016.
16. Liu L, Xu Z, Zhong L, Wang H, Jiang S, Long Q, Xu J and Guo J: Enhancer of zeste homolog 2 (EZH2) promotes tumour cell migration and invasion via epigenetic repression of E-cadherin in renal cell carcinoma. BJU Int 117: 351-362, 2016.
17. Chen X, Song N, Matsumoto K, Nanashima A, Nagayasu T, Hayashi T, Ying M, Endo D, Wu Z and Koji T: High expression of trimethylated histone H3 at lysine 27 predicts better prognosis in non-small cell lung cancer. Int J Oncol 43: 1467-1480, 2013.
18. Chen VW, Ruiz BA, Hsieh MC, Wu XC, Ries LA and Lewis DR: Analysis of stage and clinical/prognostic factors for lung cancer from SEER registries: AJCC staging and collaborative stage data collection system. Cancer 120 (Suppl 23): S3781-S3792, 2014.
19. Taira K, Hiroyasu S, Shiraishi M, Muto Y and Koji T: Role of the Fas system in liver regeneration after a partial hepatectomy in rats. Eur Surg Res 33: 334-341, 2001.
20. Fujiwara K, Fujimoto N, Tabata M, Nishii K, Matsuo K, Hotta K, Kozuki T, Aoe M, Kiura K, Ueoka H and Tanimoto M: Identification of epigenetic aberrant promoter methylation in serum DNA is useful for early detection of lung cancer. Clin Cancer Res 11: 1219-1225, 2005.
21. Shirendeb U, Hishikawa Y, Moriyama S, Win N, Thu MM, Mar KS, Khatanbaatar G, Masuzaki H and Koji T: Human papillomavirus infection and its possible correlation with p63 expression in cervical cancer in Japan, Mongolia, and Myanmar. Acta Histochem Cytochem 42: 181-190, 2009.
22. Song N, Liu J, An S, Nishino T, Hishikawa Y and Koji T: Immunohistochemical analysis of histone H3 modifications in germ cells during mouse spermatogenesis. Acta Histochem Cytochem 44: 183-190, 2011.
23. Adams JC: Heavy metal intensification of DAB-based HRP reaction product. J Histochem Cytochem 29: 775, 1981.
24. Ellinger J, Kahl P, von der Gathen J, Heukamp LC, Gütgemann I, Walter B, Hofstädter F, Bastian PJ, von Ruecker A, Müller SC and Rogenhofer S: Global histone H3K27 methylation levels are different in localized and metastatic prostate cancer. Cancer Invest 30: 92-97, 2012.
25. Gavrieli Y, Sherman Y and Ben-Sasson SA: Identification of programmed cell death in situ via specific labeling of nuclear DNA fragmentation. J Cell Biol 119: 493-501, 1992.
26. Koji T, Kondo S, Hishikawa Y, An S and Sato Y: In situ detection of methylated DNA by histo endonuclease-linked detection of methylated DNA sites: A new principle of analysis of DNA methylation. Histochem Cell Biol 130: 917-925, 2008.
27. Camp RL, Dolled-Filhart M and Rimm DL: X-tile: A new bio-informatics tool for biomarker assessment and outcome-based cut-point optimization. Clin Cancer Res 10: 7252-7259, 2004.
28. Ross JP, Rand KN and Molloy PL: Hypomethylation of repeated DNA sequences in cancer. Epigenomics 2: 245-269, 2010.
29. Digel W and Lübbert M: DNA methylation disturbances as novel therapeutic target in lung cancer: Preclinical and clinical results. Crit Rev Oncol Hematol 55: 1-11, 2005.
30. Usemann J, Ernst T, Schäfer V, Lehmberg K and Seeger K: EZH2 mutation in an adolescent with Weaver syndrome developing acute myeloid leukemia and secondary hemophagocyticlymphohistiocytosis. Am J Med Genet A 170A: 1274-1277, 2016.

31. Tiffen JC, Gunatilake D, Gallagher SJ, Gowrishankar K, Heinemann A, Cullinane C, Dutton-Regester K, Pupo GM, Strbenac D, Yang JY, *et al*: Targeting activating mutations of EZH2 leads to potent cell growth inhibition in human melanoma by derepression of tumor suppressor genes. Oncotarget 6: 27023-27036, 2015.
32. Bosselut R: Pleiotropic functions of H3K27Me3 demethylases in immune cell differentiation. Trends Immunol 37: 102-113, 2016.
33. Zhou Z, Gao J, Popovic R, Wolniak K, Parimi V, Winter JN, Licht JD and Chen YH: Strong expression of EZH2 and accumulation of trimethylated H3K27 in diffuse large B-cell lymphoma independent of cell of origin and EZH2 codon 641 mutation. Leuk Lymphoma 56: 2895-2901, 2015.
34. Vick AD and Burris HH: Epigenetics and health disparities. Curr Epidemiol Rep 4: 31-37, 2017.
35. Valeri L, Reese SL, Zhao S, Page CM, Nystad W, Coull BA and London SJ: Misclassified exposure in epigenetic mediation analyses. Does DNA methylation mediate effects of smoking on birthweight? Epigenomics 9: 253-265, 2017.
36. Tehranifar P, Wu HC, McDonald JA, Jasmine F, Santella RM, Gurvich I, Flom JD and Terry MB: Maternal cigarette smoking during pregnancy and offspring DNA methylation in midlife. Epigenetics: May 11, 2017 (Epub ahead of print).
37. Takeshima H, Wakabayashi M, Hattori N, Yamashita S and Ushijima T: Identification of coexistence of DNA methylation and H3K27me3 specifically in cancer cells as a promising target for epigenetic therapy. Carcinogenesis 36: 192-201, 2015.